

## THE EFFECT OF DISPERSOIDS ON RECRYSTALLIZATION KINETICS AND GRAIN STRUCTURE IN HOT DEFORMED AA3004

J.P. Suni\*, R. D. Doherty\*\*, P.A. Hollinshead\*, T. N. Rouns\* and R.T. Shuey\*

\* Alcoa Technical Center, Alcoa Center, PA 15069, USA

\*\* Drexel University, Philadelphia, PA 19104

### ABSTRACT

For a fixed composition and hot deformation schedule, the potency of dispersoids to inhibit recrystallization in AA3004 was altered by varying the homogenization practice and also by varying the temperature of the anneal following hot deformation. During anneals at temperatures below 300 °C, additional dispersoids precipitated. Zener drag was calculated from the dispersoid size distribution measured using FEG-SEM. The increase in dispersoid potency due to homogenization practice slowed recrystallization kinetics, but did not have a resolvable effect on recrystallized grain structure. The increase in dispersoid potency due to low temperature precipitation during annealing resulted in additional retardation of kinetics, while it increased both the size and aspect ratio of recrystallized grains. The size change is interpreted as a reduction in number of successful nuclei. The aspect ratio change is interpreted as the effect of an isotropic Zener drag on a growth velocity which is intrinsically anisotropic, due to the anisotropic orientation of subgrain boundaries.

**Keywords:** Recrystallization, kinetics, grain size, dispersoids, characterization, spectrum.

### 1. INTRODUCTION

Addition of second phase particles is well known to affect recrystallization kinetics and grain size and shape. The direction of the effect depends on circumstances. Doherty and Martin[1] first clearly showed that coarse particles speed up recrystallization, while fine particles slow it down. The size separating coarse and fine is essentially the subgrain size. Nes and others[2] showed that while coarse particles decrease grain size, addition of fine particles can either increase or decrease grain size. When the final grain size is determined by secondary grain growth, addition of fine particles reduces grain size by limiting this growth. Conversely, when final grain size is determined by primary grain growth, addition of fine particles increases grain size by reducing the number of successful nuclei. Also well known, but less investigated, is the observation that the addition of fine particles increases the aspect ratio of recrystallized grains. The present work reports and interprets some data on the effect of fine particles on recrystallization kinetics and grain dimensions in commercially hot rolled 3004.

### 2. PROCEDURE

The material used was fabricated in 1996 using two preheat practices, resulting in two different dispersoid structures. The higher temperature preheat practice is signified as "H" and the lower temperature as "L". Hot rolling conditions were similar for the two preheat conditions. Both samples were quenched edge trim at hot line exit gauge. Alloy composition, in wt% was 0.19 Si, .42 Fe, .14 Cu, 1.01 Mn and 1.22 Mg for both samples.

Dispersoid size spectra were characterized using image analysis techniques on electron photomicrographs. Backscattered electron images were collected from polished specimens at a magnification of 10000X using a Philips X130 field emission gun scanning electron microscope. An accelerating voltage of 10kV, spot size 4, and a working distance of 5 mm proved to give the best combination of both gray level and spatial resolution of these particles. These conditions yielded a lower limit of 20nm for size detection. Twenty-five fields were analyzed.

After isothermal anneals of various times and temperatures, fraction recrystallized, hardness, and recrystallized grain size were measured, all at the T/2 position. Anneals for times less than an hour were done in a molten metal bath. For longer anneals, samples were transferred to an air furnace after one hour in the molten metal bath. Fraction recrystallized was estimated from optical micrographs. Hardness measurements were made with a 3 Kg load on a Zwick Model 3212 diamond indentation (Vickers type) machine, and averages were obtained for roughly 10 measurements. Recrystallized grain sizes were measured on optical micrographs for three separate frames at 200X magnification, using the linear intercept method. Averages were obtained for roughly 10 measurements. Selected samples were tested for electrical conductivity.

### 3. CHARACTERIZATION RESULTS

Figure 1 gives the dispersoid spectra of both materials, in terms of the Zener drag parameter,  $f/r$ , or volume % divided by radius. Other spectra, such as volume percent, number per area and number per volume, look qualitatively similar to those shown in Figure 1, differing primarily in peak position and modest edge effects. Dispersoid particles were grouped by area, and each interval of particle area is labeled by the radius of an equivalent circle. The Saltykov correction[3] made for Figure 1 includes shifting a fraction of the counts to intervals of larger size, to statistically account for the circumstance that the equatorial size is the largest of a range of sectioned sizes.

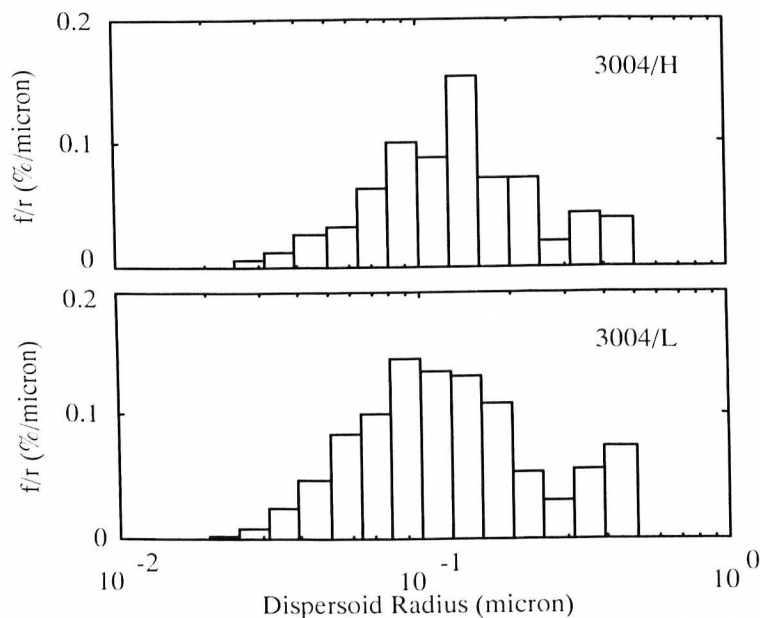


**Figure 1. Dispersoid volume percent divided by radius,  $f/r$ .**

Spectral distribution statistics are summarized in Table 1. All of the statistics indicate that the lower temperature preheat gives the more potent dispersoid structure. The estimated number of particles per volume,  $N_v$  pertains both to nucleation and to secondary grain growth. These processes involve adjustment of subgrain or grain boundaries, respectively, driven by reduction of boundary energy. This driving force is so weak that the boundary is effectively pinned by the particle. Spectral distributions (not shown) indicate that the raw value of  $N_v$  is biased low because the population has a tail extending below the resolution limit of 0.02 micron (20 nanometers). The alternative values for  $N_v$  given parenthetically in the second column of Table 1

include an estimation of the  $N_V$  contribution from the extension of the distribution to sizes below the resolution limit. The other statistics appearing in Table 1 would have significantly less correction for resolution limit, because they have less weighting of small sizes. The third column of Table 1 gives the corresponding 3D dispersoid spacing,

$$\lambda = (N_V)^{-1/3} \quad (1)$$

Table 1. Dispersoid Statistics

Alloy	$N_V$ (1/ $\mu\text{m}^3$ )	$\lambda$ ( $\mu\text{m}$ )	f (vol%)	$f_{\text{ias}}$ (vol%)	$\Sigma(f/r)$ (%/ $\mu\text{m}$ )	$r_Z$ ( $\mu\text{m}$ )	$r_A$ ( $\mu\text{m}$ )
3004/H	2.59 (4.09)	0.73 (0.62)	0.73	0.78	5.9	.12	0.085
3004/L	4.69 (4.91)	0.60 (0.59)	1.00	0.90	9.0	.11	0.076

The metallographically determined volume fraction,  $f$  given in the fourth column of Table 1, can be compared with other data on how alloying elements are distributed among phases. The next column gives the dispersoid volume percent obtained independently by combining conductivity readings with total composition and detailed constituent particle analysis. The two methods agree within 10%, and both indicate that for these samples, the lower temperature preheated sample has more dispersoid. The Zener drag on primary growth of recrystallized grains can be calculated by summing up the  $f/r$  contributions over all sizes, and values are given in Table 1 for both starting materials. Since the  $f/r$  contribution from the extreme size intervals is rather small, it is likely that the error due to undetected particles is negligible. The Zener radius  $r_Z$  given in Table 1 is the ratio of the volume fraction to the summed  $f/r$ , both determined microscopically. The area-weighted section radius  $r_A$  is the radius of a circle equal in area to the average sectioned particle area. The values of  $r_A$  are somewhat smaller than the values of  $r_Z$ , but they are of the same order of magnitude.

## 4. RESULTS

### 4.1 Recrystallization Kinetics

The results for recrystallization kinetics are given in Figure 2, where the times required for 50% recrystallization are plotted against reciprocal temperature. The 3004/L recrystallizes more slowly than 3004/H. Also, the data in Figure 2 are fairly straight and parallel at high temperature, i.e., on the left. The slope, here corresponds to an activation energy of 237 kJ/mole, which is similar to other published values for hot rolled, non-heat treatable alloys.[4-6] The effect of dispersoids on recrystallization kinetics can be estimated from the separation between the curves in Figure 2. This is roughly a factor 1.8, meaning that the high temperature preheated material achieves 50% recrystallization about 1.8 times faster.

A striking and unanticipated feature of Figure 2 is the pronounced upwards curvature of the data at low temperature, i.e., to the right. The recrystallization time is longer than would be predicted by extrapolation from high temperature using the Arrhenius relation. This was found by conductivity measurements to simply reflect additional precipitation (approximately 0.2 volume%) occurring at these low temperatures and long times. The extreme departure of the curves from the extrapolation to low temperature suggests that additional nucleation of dispersoids must be occurring during annealing, as the effect of growth on  $f/r$  would be fairly modest. The size spectra of dispersoids in the as-annealed condition were not quantified.

### 4.2 Recrystallized Grain Size

Measured grain dimensions for fully recrystallized material are given as a function of anneal temperature in Figure 3, for both the longitudinal and short transverse directions. The aspect ratio

is fairly independent of temperature, except at the lowest anneal temperature, where it is distinctly larger. The grain sizes are very close for the two 3004 preheat practices; although it could also be argued, on the basis of the highest anneal temperature data, that the grain size is smaller for 3004/H. If so, the larger grain sizes, as well as aspect ratios, correspond consistently to the longer recrystallization times and the more potent dispersoid structure.

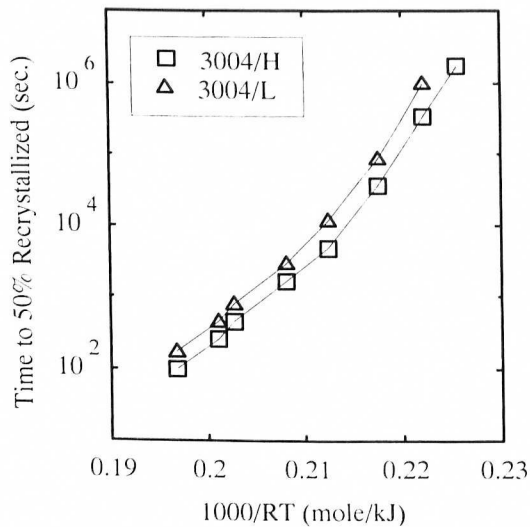


Figure 2. Time for 50% recrystallization.

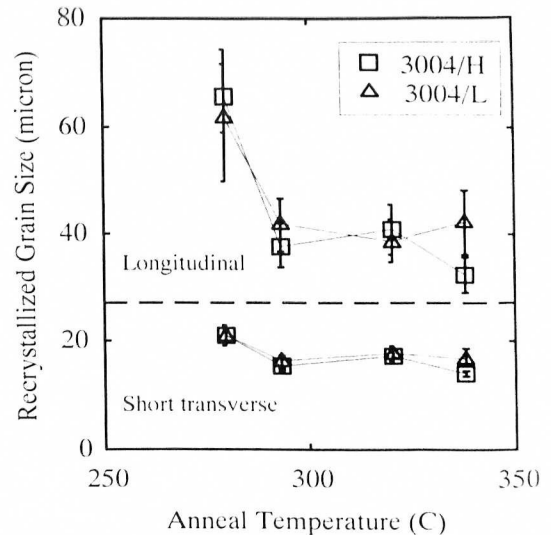


Figure 3. Recrystallized grain size, including 95% confidence bars.

Figure 3 also shows that at the lowest anneal temperature the grain sizes are larger than the size at higher temperatures. This relation of grain size with anneal temperature is opposite to that commonly cited as "Recrystallization Law #4", [7] which does not involve dispersoid effects. The additional size at low anneal temperature is primarily in the longitudinal direction. Although the data are sparse and imprecise, the larger grain size and larger aspect ratio at low temperature can be tentatively associated with the previously described anomalous long recrystallization time. All these shifts in recrystallization could be associated with stronger dispersoid influence.

## 5. DISCUSSION

### 5.1 Growth Rates

Joint analysis of recrystallization kinetics and grain size enables distinction of nucleation and growth: The recrystallized grain size indicates the spacing of successful nuclei, while the ratio of size to time indicates the rate of primary growth. Figure 4 shows the estimated rate of growth for both materials. These look qualitatively like the times to 50% recrystallization shown in Figure 2.

### 5.2 Anomalous Delay at Low Temperature

Figure 2 showed that the recrystallization time at low temperature is longer than would be predicted by extrapolation from high temperature using the Arrhenius relation. The anomalously long recrystallization time is apparently due to slowing of growth rather than delay in nucleation. This is indicated by the similarity in plots of growth rate and recrystallization time, Figures 4 and 2 respectively. The same conclusion can also be reached by considering hardness measurements. Previous work [4] indicated that for hot rolled, non-heat treatable alloys, roughly 20% recovery occurs before the onset of recrystallization. Whether there is any detectable increase in nucleation

time can be checked by plotting the time required for 20% recovery. Figure 5 shows there is no low temperature curvature in the recovery times which corresponds to the curvature in recrystallization time. A statistical F-test shows that the slope of the entire recovery plot is indistinguishable from the slope of high temperature portion (first five points) of the recrystallization plot. Hence, there is no detectable anomaly in recovery time.

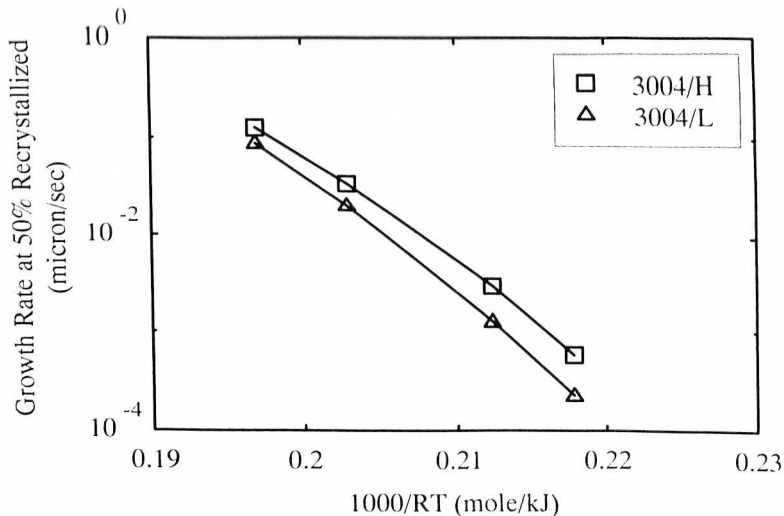


Figure 4. Estimated growth rate at 50% recrystallization.

### 5.3 Effect of Dispersoids on Grain Dimensions

While the data within this report give definite correlations of dispersoid potency with grain dimensions, they are insufficient for quantitative modeling, both in respect to magnitude of change and number of observations. However the sense of the observed correlations is as expected from the principles that would be involved in modeling. The dispersoid spacing (Table 1) is much smaller than the grain dimensions (Figure 3), so that secondary grain growth is severely limited. Increasing the dispersoid potency should then increase the grain size, as observed, by reducing the number of successful nuclei. Because nuclei are sites of exceptional rather than average strain, the observation that the average dispersoid spacing (Table 1) and average subgrain size (estimated from yield strength measurements to be roughly  $1 \mu\text{m}$ ) are about the same suggests that there should be an effect of dispersoids on grain size. To be more quantitative, a more specific model of the typical nucleation site would be needed.

The physical basis for the observed correlation of dispersoid potency with aspect ratio is more subtle. Anisotropy of recrystallized grain dimensions implies anisotropy in primary growth velocity. For spherical particles, as in the present case, the Zener drag is isotropic. Furthermore the stored energy, being a scalar, is also without orientation. A plausible mechanism for anisotropy of recrystallized grains is anisotropy in subgrain dimensions. The advancing, high angle boundary of a recrystallized grain tends locally to be at a large angle to the intersecting subgrain boundaries in the deformed substructure, due to local energy minimization. The advance of the high angle boundary is slowest in a direction perpendicular to the subgrain boundaries being consumed. The average velocity of primary grain growth is anisotropic if the deformed substructure is anisotropic, being slower in the transverse direction. Isotropic reduction in driving force by the Zener mechanism increases the ratio of velocities in the longitudinal and transverse directions of the deformed substructure.